AUTOMATED SEGMENTATION OF LUNGREGIONS BASED ON THRESHOLDING, MORPHOLOGICAL OPERATORS AND CURVATURE ANALYSIS

Madhura J

Research Scholar, Department of Computer Science and Engineering, Dayananda Sagar College of Engineering, India,
madhu-ise@dayanandasagar.edu, Orcid id-0000-0001-7490-2363

Dr. Ramesh Babu D R

Professor & Head, Department of Computer Science and Engineering, Dayananda Sagar College of Engineering, India.
hod-cse@dayanandasagar.edu

Abstract:

Segmentation of lung pleura is a pre-processing step in CAD which helps in reducing false positives in detection of lung cancer. The existing methods fail in extraction of lung regionswith the nodules at the pleura, mediastinum of the lungs. In this step, new methods are proposed which segments lung regions with nodules at the pleura, mediastinum of the lungsbased on curvature analysis and morphological operators. The proposed algorithm is testedon 150 patient's dataset which consists of 150 images of LIDC and the results are found tobe satisfactory.

Introduction

Early detection and classification of lung cancer tumors (nodules) is an active research area in medical image processing domain, because it is still an unsolved challenging task. Segmentation of lung regions is a preprocessing step in CAD, which takes less computational time for the detection of lung cancer. It is strenuous for the radiologiststo diagnose the cancer, when the lung nodules are attached to the pleura (lung border) andmediastinum (middle portion of the chest) of the chest. The existing algorithms [1,2] fail to segment the lung regions with nodules attached to the mediastinum and pleura of lung regions. In this research work, algorithms are proposed to automate the process of segmentation of the lung regions with nodules attached at the pleura and the mediastinum of the lungs using curvature analysis, active contour, thresholding and morphological operators thereby assisting the radiologists.

Related Work

Thresholding method is not suitable for the segmentation of tumor which is attached to mediastinum of the lungs [3]. Yoshinori Itai et al. [4] have applied active contour model to locate the contour of the object which in turn segmented lung fields, but the drawback of active contour [80] is the design of initial mask which needs manual interaction and alsoiterations are to be given to extract the desired object. Yang Liu et al. [5] and Nihad Mesanovic et al. [1] have suggested region growing algorithm to extract lung areas and the restriction of region growing is its performance which depends on initial seeds and also computationally intense. Amjed S. Al-

Fahoum et al. [6] have extracted lungs using threshold and labelling operations and Zhaoxue Chen et al. [7] used image threshold, fast flood filling technique, erosion operation and an area-filtering step to extract lungs. Diao Liming et al. [8] have applied optimal threshold value, boundary tracking and mathematical morphology method to extract lungs.

Hu et al. [9] have used threshold, region growing, component labeling and morphological processing for the segmentation of lungs. I. Sluimer, S. Diciooti, Armato S G have implemented rolling ball algorithm [10-12] to get lung tumorsconnected to the walls of the lungs but this approach has the drawback of fix size for the structuring element used forfilling the tumors at the walls. Jun Lai et al. [88] have segmented the lung regions along thenodules at the border using active contour with prior shape to fit the boundary of lung field.As per the survey, extraction of lung regions with the nodules at mediastinum and pleura is challenging. In this direction, an attempt is made to extract the lungs with the tumors attached at the mediastinum of the lungs and pleura of the lungs which is discussed in the proposed method. The proposed algorithms are compared with the existing algorithms andthe results are found to be satisfactory.

Proposed Method

In the proposed algorithms, segmentation of lung regions with nodules attached to the wallof the lungs whose size is smaller or bigger and those nodules attached to the mediastinumof the lungs are taken into consideration.

The proposed segmentation algorithm 1.1, segments nodules attached to the wall of the lung region based on thresholding and morphological operations. Thresholding technique is used to remove the background of the image using equation (1.1).

$$binary(i, j) = \begin{cases} 1, & if\ f(i, j) < T \\ 0, & otherwise \end{cases}$$

(1.1)

where T is -420 HU [13], $binary(i, j)$ is the binary image obtained after applyingthresholding.

Image outline is delineated and are cleared to remove the regions which are connected to

the borders of the image [14] using equation (1.2).

$$R = \begin{cases} 0, & border(R) = B\ pixels \\ 1, & border(R)\ /= B\ pixels \end{cases}$$

(1.2)

Where R represents regions with different labels. B represents those pixels which are at theborder of the image.

Closure operation is performed to close the small distorted area (region of the lung CT image where the borders are not complete and broken) which are at the borders of the lungsusing a disk shaped structuring element using equation (1.3).

$$A \cdot B = (A \oplus B) g B \quad\quad\quad (1.3)$$

Where A is the input image and B is the structuring element.

Areas of all Connected Components (CC) of the image are computed and the two largest CC are extracted (whose areas are more than remaining areas of CC) using equation (1.4) to get lung mask.

$$Lungregion = \begin{cases} \max \ (area(R)) & lung1 \\ (max-1)(area(R)) & lung2 \end{cases} \quad\quad (1$$

Whereas max is the maximum, area(R) is the area of the CC,(max-1) is the (maximum-1),lung 1 and lung 2 are two lungs i.e. left lung and right lung.

The closure operation with the disk structuring element [15] is performed on lung mask to include the nodules inside the lungs. The holes inside the two connected components are filled using equation (1.3). The resultant image is superimposed with the given original image to extract lung regions. The borders of the lung regions are then smoothened for proper segmentation using erosion operation by making use of equation (1.5).

$$A \, g B = \{ z | (B) z \subseteq A \} \quad\quad\quad (1.5)$$

A is the reference binary image, B is the disk shaped structuring element and z is the outcome element of the equation (1.5).

In the next step, eroded image is subtracted from the reference binary image using (1.6).

$$S = A - z \quad\quad\quad (1.6)$$

S contains image which has smooth borders.

Algorithm 1.1 Pseudo code for the segmentation of lung regions using morphological Operators

Input: DICOM CT Image**Output:** Lung Regions **Method:**

Step 1: Thresholding is used to remove background of the image.

Step 2: Connected Components (CC) are labeled using run-length encoding to identify different CC.

Step 3: Clear borders and morphological closure operations are used to extract lung maskStep 4: The two largest connected components is extracted to create the mask of lung

regions

Step 5: Morphological closure operations are used to include the nodules attached to wallsof the lungs and fill the lung regions to get lung mask

Step 6: Superimpose lung mask on the input image to segment lung regions

Step 7: Smoothen the borders of the image by eroding the image with the disk shaped structuring element. The eroded image is subtracted from the binary image.

Algorithm 1.1 uses intensity values to generate a mask, but for few images, intensity valuecannot be used as the parameter to obtain the mask. Therefore, to overcome this problem a new method based on active contour and edge detector is proposed to extract the lung regions. Canny edge detector is used to get the edges of the DICOM CT image and then active contour is applied on the image with different edges using equation (1.7).

Unwantedborders of the image are cleared to get different connected components and the two largestconnected components are extracted. The gaps inside the connected components are filled in order to obtain a mask.Superimpose the mask over the original DICOM CT image to extract two lung regions.

$$E_{snake}[14] = \frac{\int_0^1 E_{snake}(v(s))ds \text{ which is equal to}}{F}$$

$$\int_0^1 E_{int}(v(s)) + E_{image}(v(s)) + E_{con}(v(s))ds \tag{3.7}$$

Where E_{int} represents the internal energy of the spline due to bending, E_{image} gives rise to the image forces, and Econ gives rise to the external constraint forces. E_{snake} represents snake energy.

Algorithm1.2 Pseudo code for the segmentation of lung regions using active contour and

morphological operators

Input: DICOM CT Image**Output:** Lung Regions **Method:**

Step 1: Initial lung regions mask is extracted using canny edge detector and active contour.

Step 2: Connected Components (CC) are labeled using run-length encoding to identify different CCs.

Step 3: Image borders are cleared to get different connected components.

Step 4: The two connected components which contain more pixels are extracted and theholes inside the connected components are filled.

Step 5: Morphological closure operation is applied to include nodules attached to theborder of the lungs.

Step 6: Superimpose the mask over the input DICOM CT image to get lung regions.

Algorithm 1.1 and 1.2 cannot segment small sized nodules and nodules attached to the walls of the lungs. The drawbacks of algorithm 1.1 and 1.2 are overcome by the use of curvature analysis and morphological operators to extract the lung regions with nodules atthe pleura. The first step is to segment the lung region using threshold technique [15] and then find the largest connected components. If the curvature of lung parenchyma is more than the curvature at the mediastinum, perform the following steps: Centroid of the lung regions is calculated and then compute the distance between centroid and boundary pixelsof the lung regions using (1.8) as shown in the figure 1.1.

Let $c(x,y)$ is the centriod and $p_i(x,y)$'s are the points on the border of the lung where $i = 1,2,...,n$

$$D_i = \sqrt{[c(x)-p_i(x)]^2 + [c(y)-p_i(y)]^2} \qquad (1.8)$$

The curvature whose difference value of two consecutive distances is more is extracted using (1.9), join the end points of curvature to extract the nodule which are attached to thelung pleura.

The distance from centroid to each point on the border is calculated using

$$E_k = D_{i+1} - D_i \qquad (1.9)$$

Where E_k is the differences between the two consecutive distances, $k = 1, 2, . . . , -1$. Q_a and Q_b in figure 1.1 are two points which has more difference value, which is to be joinedfor further processes. The extracted nodule is added with missing nodule at the pleuraof the lungs to extract two lung regions. In figure 1.2 shows the difference between two

consecutive distances where A* refers angles from centroid to the border points.

If the curvature of lung parenchyma is less than the curvature at the mediastinum, performthe

following steps: find the largest connected components whose area is more and superimpose the extracted lungs over the input image. Convex Hull and XOR operation are performed to get the mask and superimpose the mask over the input image to extract lung regions.
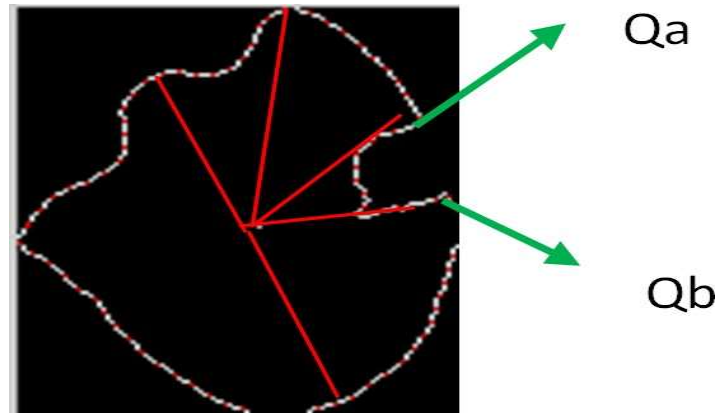

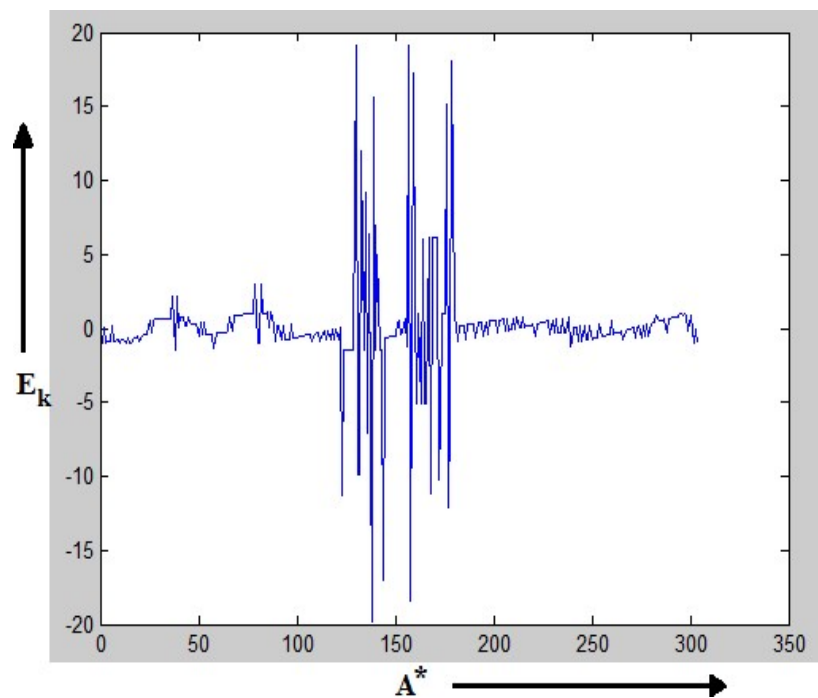**Figure 3.1:** Euclidean distance between centriod and border points

Figure 3.2: Graph shows difference between two consecutive distances

---

Algorithm 1.3 Pseudo code for the segmentation of lung regions using curvature analysis

Input: DICOM CT Image**Output:** Lung Regions **Method:**

Step 1: Lung regions are extracted based on threshold method and the various connected components are labeled using run length encode.

Step 2: Based on the area calculation largest connected components are extracted and the curvature of the lung region is analyzed on the basis of the following cases:

Case 1: If the curvature at mediastinum is less when compared to the curvature atthe pleura, then apply the following steps on each lung region:

(i) Calculate the centroid of the lung regions and calculate the distancebetween centroid and boundary pixels of the lung regions.

(ii) The curvature where the difference value of two consecutive distance is more is extracted, end points of curvature are joined to extract the nodule that are attached to the lung pleura.

(iii) The extracted nodule is added with missing nodule at the pleura of the lungs to extract two lung regions.

Case 2: Convex hull is applied if the curvature is more at mediastinum and then XOR operation is applied to extract those lung nodules that are attached to the lung pleura.

Algorithm 1.3 doesn't segment those nodules which are attached to the mediastinum of thelungs. Algorithm 1.4 overcomes the drawbacks of algorithm 1.3. The proposed method makes use of curvature analysis and morphological operators to extract lung regions with nodules at mediastinum.

The first step is to segment the lung regions using threshold technique [15] and to find the largest connected components. Here, lung regions are extracted without the lung nodules at the mediastinum of lungs. This is as shown in the figure 1.3(b).The lungs whose nodules are not attached to the wall of the lungs are extracted. This is as shown in the figure 1.3(c). Convex hull is applied on the lung regions, XOR operation is performed between convex hull image and figure 1.3(c). The connected component whosearea is more is extracted. This is as shown in the figure 1.3(d).
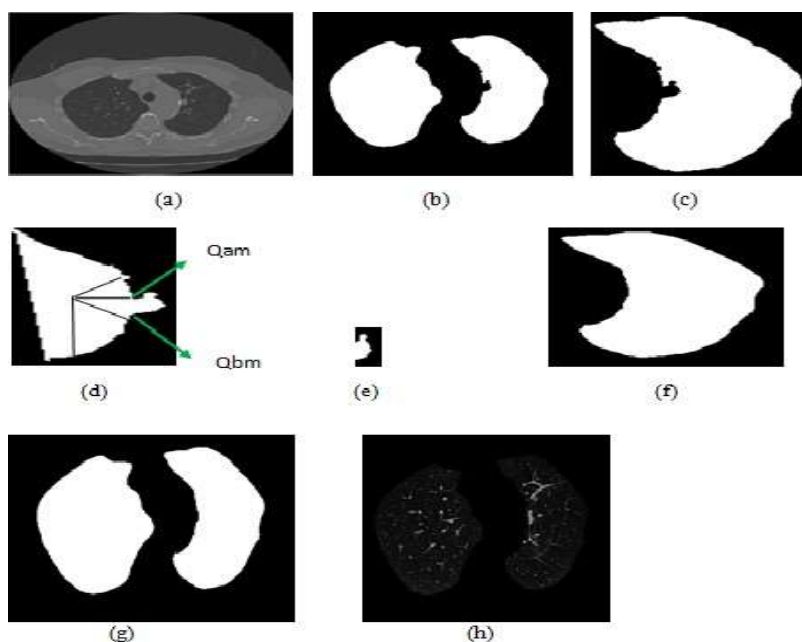
Figure 1.3: (a) DICOM input Image (b) Initial lung mask (c) Extraction of lung region without lung nodule at the mediastinum of lungs (d) Euclidean distance between centriod and border points (e) Extraction of lung nodule (f) Extraction oflung region with lung nodule at the mediastinum of lungs (g) Lung Mask with nodules at the borders (h) Extraction of lung regions

Let *Qam* and *Qbm* in figure 1.3(d) be the two points which has more difference value, which is to be used to cut the nodule. The extracted nodule is as shown in the figure 1.3(e)is removed from the figure 1.3(d). The extracted nodule is attached to the figure 1.3(c) to get the lung region with the nodule as shown in the figure 1.3(f). The extracted lung regionsact as the mask. This is shown in the figure 1.3(g). The mask is superimposed over the input image to extract lung regions. This is shown in the figure 1.3(h). The segmentation of lungregions is explained in algorithm 1.4.

Algorithm 1.4 Pseudo code for the segmentation of lung regions using curve analysis and morphological operators

Input: DICOM CT Image**Output:** Lung Regions **Method:**

Step 1: Lung regions are extracted based on active contour method and various connected components are labeled using run length encode.

Step 2: Largest connected components are calculated based on area calculation and then following steps are applied on each region:

(i) Convex hull and XOR operations are applied to extract the connectedcomponents.

(ii) The connected components with more area are considered and the centroid of those connected components are found. The distance between centroid and boundary pixels of the lung regions are calculated.

(iii) The curvature of the two consecutive distances whose difference values aremore are extracted and the region attached to the mediastinum are extracted.

(iv) The extracted nodule is added with missing nodule at the mediastinum of thelungs to extract two lung regions.

Results and Discussions

For analysis and validation of the proposed method, totally 150 images are considered. Among these 150, 10 images containing nodules of different kinds are taken for experimentation purpose. In order to compare the proposed system with the segmentation techniques listed in the literature, performance metric Jaccard similarity coefficient (Overlap measure) [16] is used. The detail result comparisons of 10 images are presented here as sample.

Overlap measure is the agreement between the ground truth (GT) and the estimated segmentation mask (S) which is given by (1.10).

$$\Omega = \frac{|S \cap GT|}{|S \cup GT|} = \frac{|TP|}{|FP| + |TP| + |FN|} \quad (1.10)$$

where TP (True Positives) represents correctly classified pixels, FP (False Positives) represents pixels that are classified as object but that are in fact background, and FN (False Negatives) represents pixels that are classified as background but that are in fact part of the object. The average overlap ($A\Omega$) measure in % can be calculated by using (1.11).

$$A\Omega = \frac{(\Omega_1 + \Omega_2 + \Omega_3 + \cdots + \Omega_n)}{n} \quad (1.11)$$

Where Ω_i is the overlap measure for each image, $i = 1$ to n and n is the total number of images.

Algorithm 1.1 uses thresholding, morphological operators and an initial mask is generated based on intensity value. The figure 1.4 shows the results obtained after applying algorithm 1.1 in which 1.4(a) is the input DICOM image, 1.4(b) shows the lungs using region-growing, 1.4(c) shows the lungs using active contour and 1.4(d) depicts the lungs using proposed method.
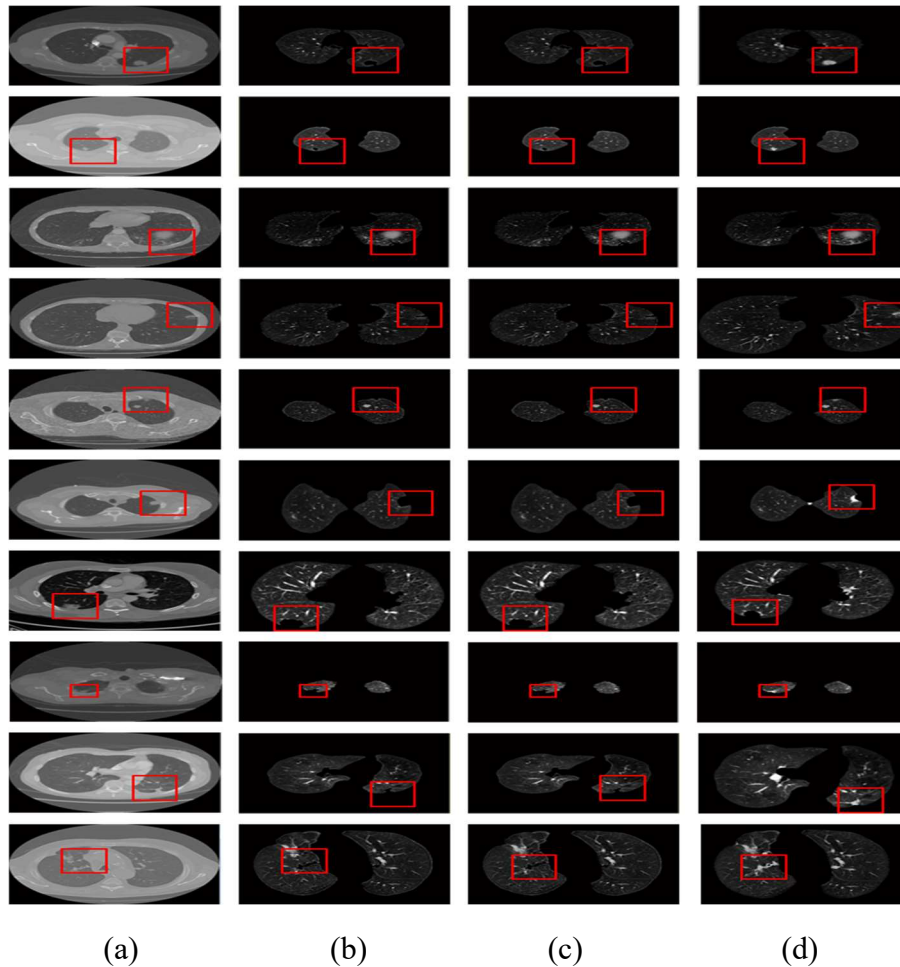

(a)   (b)   (c)   (d)

Figure 1.4: (a) DICOM CT image (b) Segmentation of lung regions using Region-Growing [1] (c) Segmentation of lung regions using Active contour [17] (d) Proposed System for the segmentation of lung regions

The overlap measure (Ω) for the proposed method (algorithm 1.1), active contour and

region growing methods are as shown in the table 1.1. The box and whiskers plot for the table 1.1 is shown in the figure 1.5, where the x-axis shows methods and y-axis shows Ω. The error rate produced by the proposed algorithm is lesser when compared to Active contour and region growing methods. Accuracy of segmentation of lung regions increases as error rate decreases. Thereby it can be concluded that the proposed method gives better results compared to the active contour and the region growing methods.

Table 3.1: Overlap Measures of Region-Growing, Active Contour and Proposed Method (Algorithm 1.1)

| Image No	Image ID	Region Growing [9]	Active Contour[80]	Proposed Method (Algorithm 3.1)
1	Image-0002	0.960	0.960	0.980
2	Image-0006	0.950	0.950	0.980
3	Image-0008	0.960	0.960	0.980
4	Image-0010	0.970	0.970	0.990
5	Image-0012	0.970	0.970	0.990
6	Image-0014	0.950	0.950	0.970
7	Image-0016	0.950	0.950	0.955
8	Image-0018	0.950	0.950	0.970
9	Image-0020	0.960	0.960	0.980
10	Image-0022	0.955	0.955	0.990

Distribution of Overlap Measure(Algorithm 3.1)
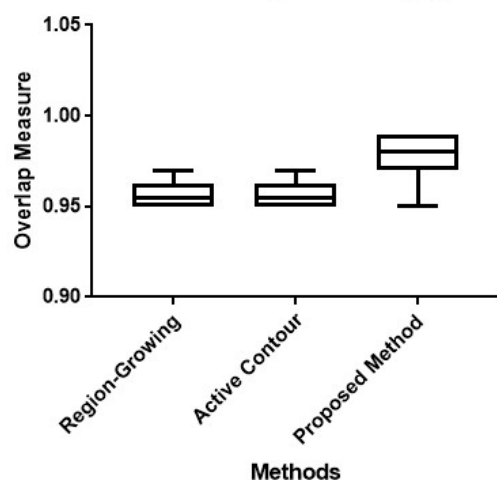
Figure 1.5: Box and whiskers plot shows the comparative study between existingmethods and proposed method with Ω

The average overlap measure ($A\Omega$) for the proposed method (algorithm 1.1, active contour and region growing methods are as shown in the table 1.2.

Table 1.2: Average Overlap Measures of Region-Growing, Active Contour andProposed Method (Algorithm 1.1)

Sl. No	AΩRegion-Growing [9]	AΩActive Contour [80]	AΩ Proposed System
1	95	95	98

Algorithm 1.1 uses intensity values to generate a mask, but for few images intensity valuecannot be used as the parameter to obtain the mask. For certain images this won't work. There by, algorithm 1.2 is used to segment the lung regions. Edge detection, active contour and morphological operators are used in algorithm 1.1. The figure 1.6 shows the results of10 images after applying algorithm 1.2. Figure 1.6(a) shows the input image. Figure 1.6(b)shows the segmentation of lung regions using region growing. Figure 1.6(c) shows the lungregions that are segmented using active contour method. Figure 1.6(d) shows the results obtained after applying the proposed method.
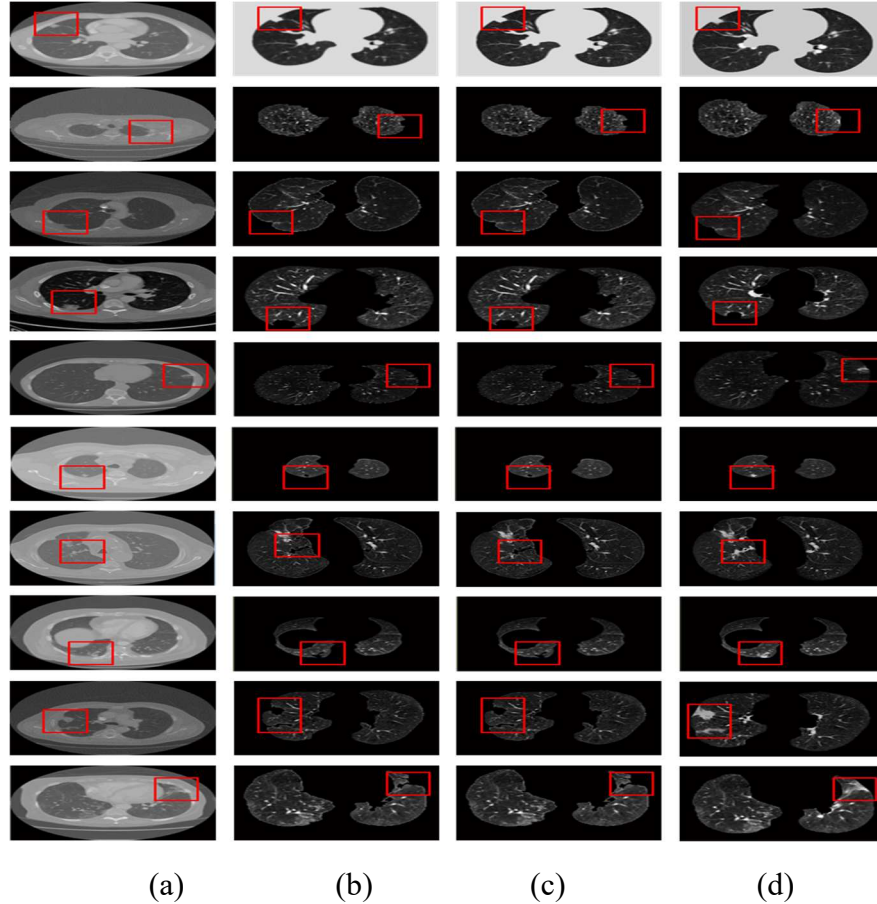
(a)   (b)   (c)   (d)

Figure 1.6: (a) DICOM CT image (b) Segmentation of lung regions using Region-Growing [9] (c) Segmentation of lung regions using Active Contour [80] (d) Proposed System for the segmentation of lung regions

Table 1.3 contains the values of the overlap measure (Ω) for the region growing method, active contour method and proposed method (Algorithm 1.2). The proposed method produces lesser error rate when compared to active contour and region growing methods. The box and whisker plot for the table 1.3 is as shown in the figure 1.7, where the x-axis represents methods and y-axis represents Ω.

Table 3.3: Overlap Measures of Region-Growing, Active Contour and ProposedMethod (Algorithm 1.2)

Image No	Image ID	Region Growing [9]	Active Contour [80]	Proposed Method (Algorithm1.2)
1	Image-0001	0.95	0.95	0.99
2	Image-0003	0.95	0.95	0.98
3	Image-0005	0.96	0.96	0.97
4	Image-0016	0.95	0.95	0.98

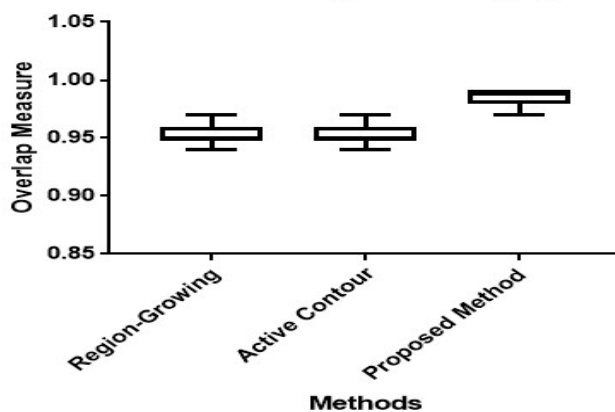| 5 | Image-0010 | 0.96 | 0.96 | 0.99 |
6	Image-0006	0.95	0.95	0.99
7	Image-0022	0.94	0.94	0.99
8	Image-0015	0.94	0.94	0.99
9	Image-0017	0.96	0.96	0.98
10	Image-0019	0.97	0.97	0.99

Figure 1.7: Box and whiskers plot shows the comparative study between existingmethods and proposed method with Ω

Table 1.4 contains the values of the average overlap measure ($A\Omega$) for the proposed method (Algorithm1.2), active contour and region growing methods. The box and whiskers plot for the table 1.4 is shown in the figure 8, where x-axis shows methods and y-axis shows$A\Omega$. The $A\Omega$ for the proposed method is comparatively better than existing methods.

Table 1.4: Average Overlap Measures of Region-Growing, Active Contour andProposed Method (Algorithm 1.2)

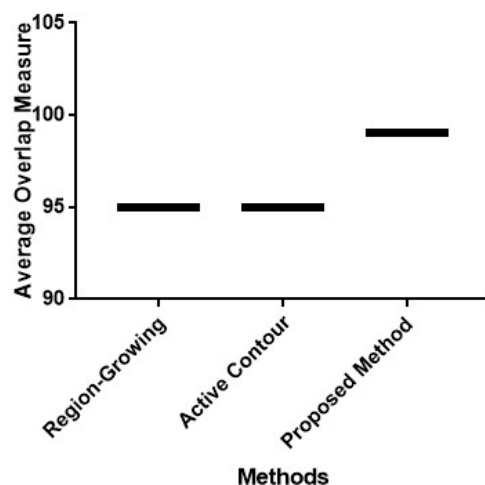| Sl. No	$A\Omega$ Region-Growing [9]	$A\Omega$ Active Contour [80]	$A\Omega$ Proposed System
1	95	95	99

Figure 1.8: Box and whiskers plot shows the comparative study between existingmethods and proposed method with AΩ

Algorithm 1.1 and 1.2 cannot segment those nodules where the number of pixels in the nodules is greater than 70 and if the nodule is attached to the walls of the lungs. The drawbacks of algorithm 1.1 and 1.2 are overcome by algorithm 1.3. Algorithm 1.3 is usedto segment the nodules attached to the walls of the lungs and whose number of pixelsare more than 70. Algorithm 1.3 fills the gap created because of the distorted borders. Once the distorted borders are filled nodules can be segmented out. Figure 1.9 shows the results of 8 images obtained after applying algorithm 1.3. Figure 9(a) depicts input DICOM CT image. Figure 9(b) shows the results of segmented lung regions obtained after applying Region-Growing method. Figure 1.9(c) shows the output obtained after applying Morphological Operators and figure 1.9(d) shows the results produced by the Proposed System.
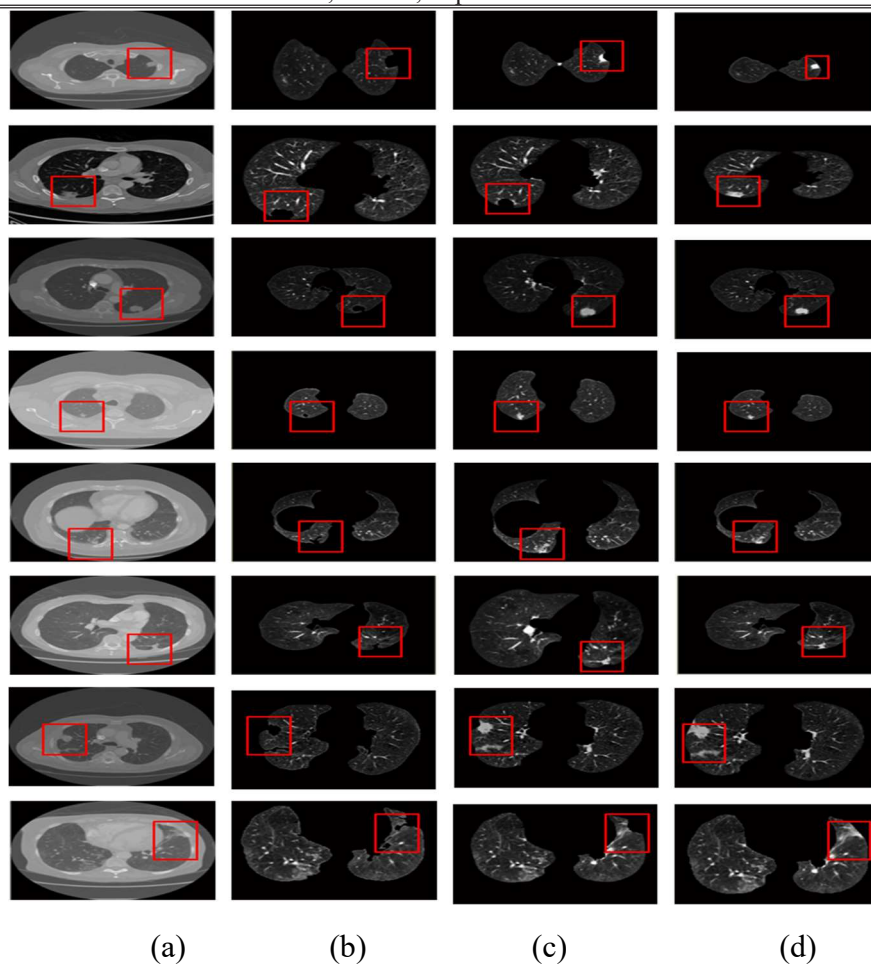
(a)	(b)	(c)	(d)

Figure 1.9: (a) DICOM CT image (b) Segmentation of lung regions using Region-Growing [1] (c) Segmentation of lung regions using Morphological Operators [2] (d) Proposed System for the segmentation of lung regions

Table 1.5 contains the values of the overlap measure (Ω) for the proposed method(algorithm 1.3), region growing and active contour methods. The proposed method produces better error rate than the existing methods. The box and whiskers plot for the table 1.5 is shown in the figure 1.10, where the x-axis depicts the methods and the y-axis depicts Ω.

Table 1.5: Overlap Measures of Region-Growing, Morphological Operators andProposed Method (Algorithm 1.3)

Image No	Image ID	Region Growing [9]	Morphological Operators [79]	Proposed Method (Algorithm 1.3)
1	Image-0023	0.950	0.970	0.990
2	Image-0016	0.950	0.955	0.980
3	Image-0002	0.960	0.970	0.970
4	Image-0006	0.950	0.980	0.980

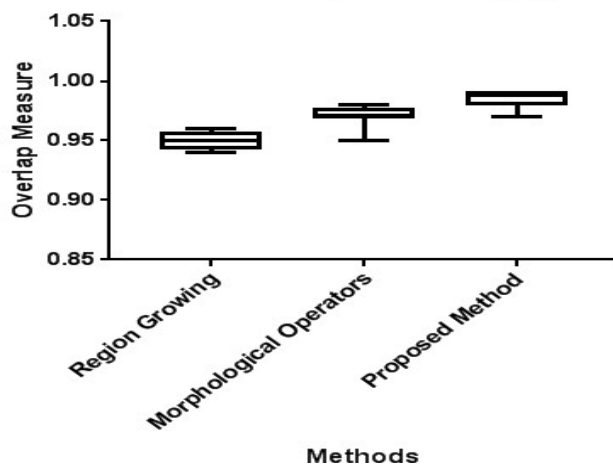| 5 | Image-0015 | 0.960 | 0.979 | 0.990 |
6	Image-0039	0.950	0.977	0.990
7	Image-0017	0.940	0.980	0.990
8	Image-0019	0.940	0.970	0.990

Figure 1.10: Box and Whiskers Plot shows the Comparative study between existingmethods and proposed method with Ω

The average overlap measure ($A\Omega$) for the active contour method, region growing method,the proposed method (algorithm 1.3) are as shown in the table 1.6. The box and whiskers plot for the table 1.6 is shown in the figure 1.11, where x-axis shows methods and y-axis shows AΩ. The AΩ for the proposed method gives better results when compare to existing methods.

Table 1.6: Overlap Measures of Region-Growing, Morphological Operators andProposed Method (Algorithm 1.3)

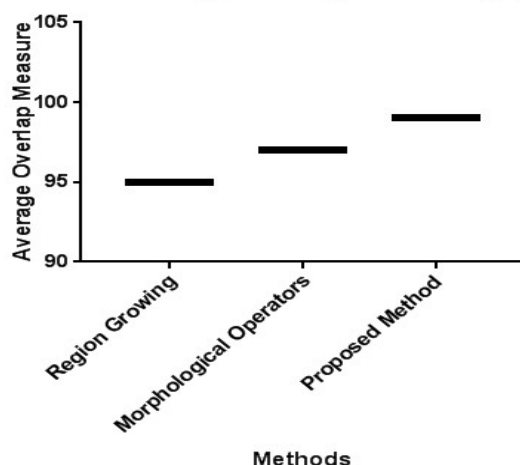| Sl. No	AΩ Region-Growing [9]	AΩ Morphological Operators [79]	AΩ Proposed System
1	95	97	99

Distribution of Average Overlap Measure (Algorithm 3.3)

Figure 1.11: Box and Whiskers Plot shows the Comparative study between existingmethods and proposed method with $A\Omega$

Algorithm 1.3 doesn't segment those nodules which are attached to the mediastinum ofthe lungs. Algorithm 1.4 overcomes the drawbacks of algorithm 1.3. Algorithm 1.4uses curvature analysis to segment the lung regions where the nodules are attached tothe mediastinum. The figure 1.13 shows the results of 7 images obtained after applying algorithm 1.4. Input DICOM image is shown by the figure 1.12(a), results of segmentationof lungs using region growing is shown by the figure 1.12(b), results of morphological operators is shown by the figure 1.12(c) and results of the proposed method is shown by thefigure 1.12(d).
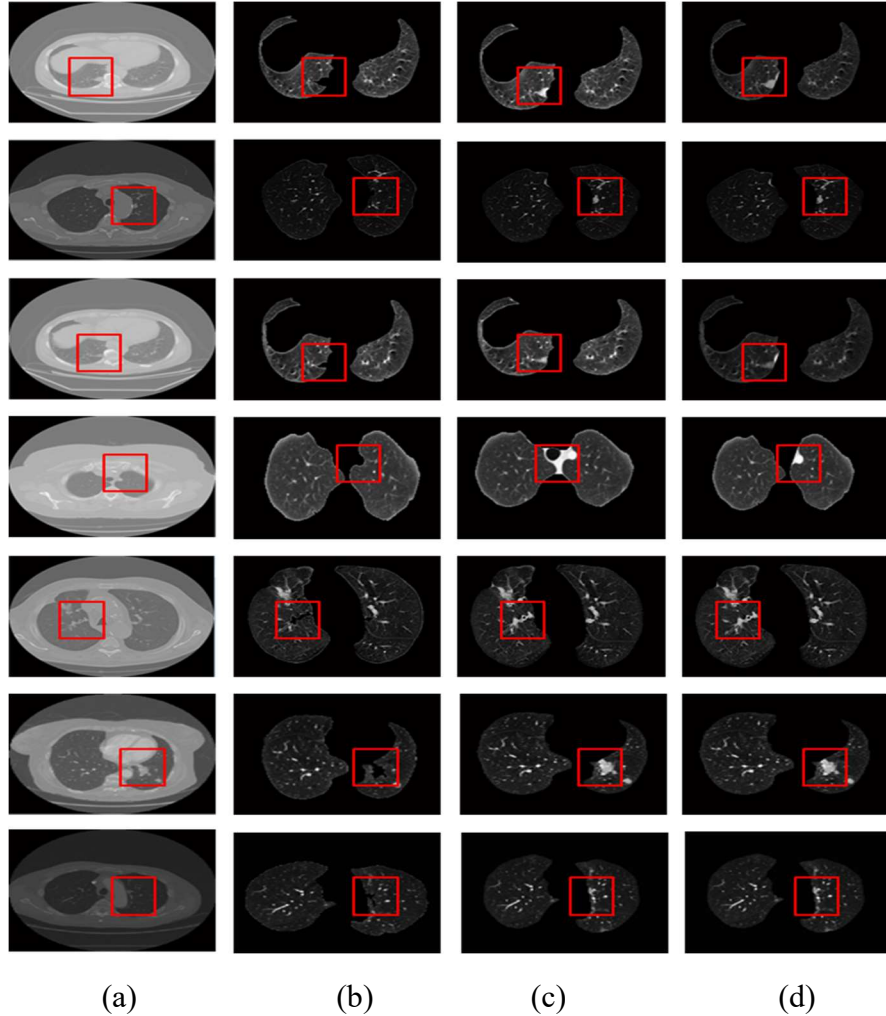
(a)   (b)   (c)   (d)

Figure 1.12: (a) DICOM CT image (b) Segmentation of lung regions using Region-Growing [1] (c) Segmentation of lung regions using Morphological Operators [2](d) Proposed System for the segmentation of lung regions

The overlap measure (Ω) for the region growing method, active contour method and proposed method (algorithm 1.4), are given in the table 1.7. Using the obtained overlap measure values a box plot is drawn. This box plot is shown in figure 1.13. The error rate produced by the proposed algorithm is lesser when compared to active contour and regiongrowing methods.

Table 1.7: Overlap Measures of Region-Growing, Morphological Operators andProposed Method (Algorithm 3.4)

Image No	Image ID	Region-Growing [9]	Morphological Operators [79]	Proposed Method (Algorithm 3.4)
1	Image-0050	0.930	0.970	0.990
2	Image-0052	0.950	0.990	0.990
3	Image-0059	0.940	0.980	0.990

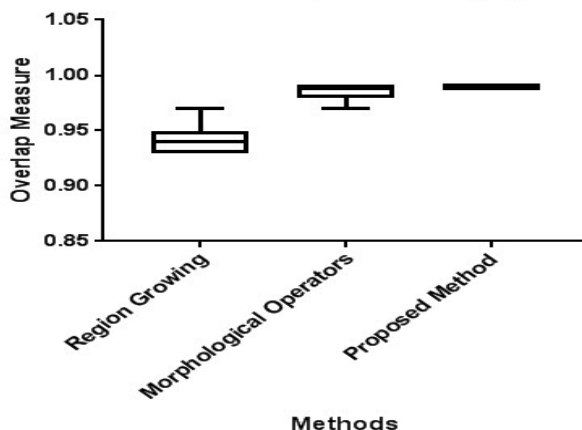|				
4	Image-0067	0.940	0.990	0.990
5	Image-0069	0.930	0.990	0.990
6	Image-0078	0.950	0.990	0.990
7	Image-0080	0.970	0.990	0.990

Figure 1.13: Box and Whiskers Plot shows the Comparative study between existingmethods and proposed method with Ω

The average overlap measure (AΩ) produced by the active contour, region growing and the proposed method (algorithm 1.4), is as shown in the table 1.8. The box and whiskers plot for the table 1.8 is as shown in the figure 1.14, here x-axis shows methods and y-axis shows AΩ. The AΩ for the proposed method gives better results when compare to existing methods.

Table 1.8: Average Overlap Measures of Region-Growing, Morphological Operatorsand Proposed Method (Algorithm 1.4)

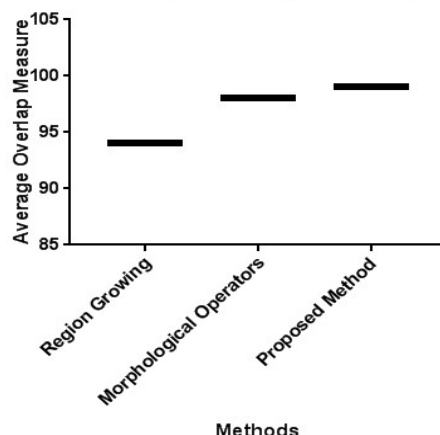| Sl. No	AΩ Region-Growing [9]	AΩ Morphological Operators [79]	AΩ Proposed System
1	94	98	99

Figure 1.14: Box and Whiskers Plot shows the Comparative study between existingmethods and proposed method with AΩ

3.1 Summary

Nihad Mrsanovic et al. [9] used region growing technique which cannot segment the nodules attached to the borders of the lung image. The thresholding and morphological operator's techniques are used to segment the lung regions along with nodules which are attached to lung borders of the image. The average accuracy of the proposed method is found to be 98% when compared to the average accuracy of the existing methods [9, 79] which are 95% and 95% respectively.

As the thresholding and morphological operator's techniques use intensity values to obtaina mask, they fail to segment the lung regions. Therefore, edge detector, active contour andmorphological operator's techniques are used to segment the lung regions. The proposed method produces an average accuracy of about 99%, where as the existing methods i.e., region growing and active contour methods produces an average accuracy of about 95% each.

References

1. Z. Li *et al.*, "Low-dose CT image denoising with improving WGAN and hybrid loss function," *Comput Math Methods Med*, vol. 20, 2021
2. W. Zhu, C. Liu, W. Fan, and X. Xie, "Deeplung: Deep 3d dual path nets for automated pulmonary nodule detection and classification," in *2018 IEEE winter conference on applications of computer vision (WACV)*, IEEE, 2018, pp. 673–681.
3. K.-Y. Chiu and S.-F. Lin, "Lane detection using color-based segmentation," in *IEEE Proceedings. Intelligent Vehicles Symposium, 2005.*, IEEE, 2005, pp. 706–711.
4. M. Diwakar *et al.*, "Low-Dose COVID-19 CT Image Denoising Using CNN and its Method Noise Thresholding.," *Curr Med Imaging*, 2022.
5. J. Hu, L. Shen, and G. Sun, "Squeeze-and-excitation networks," in *Proceedings of the IEEE conference on computer vision and pattern recognition*, 2018, pp. 7132–7141.

6. O. S. Al-Kadi and D. Watson, "Texture analysis of aggressive and nonaggressive lung tumor CE CT images," *IEEE Trans Biomed Eng*, vol. 55, no. 7, pp. 1822–1830, 2008.

7. Y. Wang, X. Gao, X. Ru, P. Sun, and J. Wang, "The Weight-Based Feature Selection (WBFS) Algorithm Classifies Lung Cancer Subtypes Using Proteomic Data," *Entropy*, vol. 25, no. 7, p. 1003, 2023.

8. B. Kim, M. Han, H. Shim, and J. Baek, "A performance comparison of convolutional neural network-based image denoising methods: The effect of loss functions on low-dose CT images," *Med Phys*, vol. 46, no. 9, pp. 3906–3923, 2019.

9. W.-C. Shen, R.-F. Chang, W. K. Moon, Y.-H. Chou, and C.-S. Huang, "Breast ultrasound computer-aided diagnosis using BI-RADS features," *Acad Radiol*, vol. 14, no. 8, pp. 928–939, 2007.

10. S. Iwano, T. Nakamura, Y. Kamioka, and T. Ishigaki, "Computer-aided diagnosis: a shape classification of pulmonary nodules imaged by high-resolution CT," *Computerized Medical Imaging and Graphics*, vol. 29, no. 7, pp. 565–570, 2005.

11. El-Baz *et al.*, "Computer-aided diagnosis systems for lung cancer: challenges and methodologies," *Int J Biomed Imaging*, vol. 2013, 2013.

12. S. K. V. Anand, "Segmentation coupled textural feature classification for lung tumor prediction," in *2010 International Conference on Communication Control and Computing Technologies*, IEEE, 2010, pp. 518–524.

13. Z. Chen, C. Niu, G. Wang, and H. Shan, "LIT-Former: Linking In-plane and Through-plane Transformers for Simultaneous CT Image Denoising and Deblurring," *arXiv preprint arXiv:2302.10630*, 2023.

14. K. Suzuki, S. G. Armato III, F. Li, S. Sone, and K. Doi, "Massive training artificial neural network (MTANN) for reduction of false positives in computerized detection of lung nodules in low-dose computed tomography," *Med Phys*, vol. 30, no. 7, pp. 1602–1617, 2003

15. Keleş, A. Keleş, and U. Yavuz, "Expert system based on neuro-fuzzy rules for diagnosis breast cancer," *Expert Syst Appl*, vol. 38, no. 5, pp. 5719–5726, 2011, doi: https://doi.org/10.1016/j.eswa.2010.10.061.

16. J. Jiang *et al.*, "Multiple resolution residually connected feature streams for automatic lung tumor segmentation from CT images," *IEEE Trans Med Imaging*, vol. 38, no. 1, pp. 134–144, 2018.

17. H. Peng, H. Sun, and Y. Guo, "3D multi-scale deep convolutional neural networks for pulmonary nodule detection," *PLoS One*, vol. 16, no. 1, p. e0244406, 2021.